

Itinerant antiferromagnetism in the Mott compound $V_{1.973}O_3$

Wei Bao

Brookhaven National Laboratory, Upton, New York 11973 and Johns Hopkins University, Baltimore, Maryland 21218

C. Broholm

Johns Hopkins University, Baltimore, Maryland 21218

and National Institute of Standards and Technology, Gaithersburg, Maryland 20899

J. M. Honig and P. Metcalf

Purdue University, West Lafayette, Indiana 47907

S. F. Trevino

United States Army Research Laboratory, Adelphi, Maryland 20783

and National Institute of Standards and Technology, Gaithersburg, Maryland 20899

(Received 22 May 1996)

The doping-induced metallic state of the Mott system $V_{2-y}O_3$ has spin-density-wave order for $T < T_N \approx 9$ K. Dynamic spin correlations in such a cation-deficient sample, $V_{1.973}O_3$, were measured with inelastic neutron scattering throughout the Brillouin zone for energies up to $\sim 20k_B T_N$ and temperatures up to $\sim 20T_N$. The dynamic spin-correlation function, $S(\mathbf{q}, \omega)$, consists of a single ridge as a function of $\hbar\omega$ centered at each antiferromagnetic Bragg point. The \mathbf{q} , ω , and T dependence of magnetic fluctuations can be described by the self-consistent renormalization theory for weak itinerant antiferromagnets developed by Moriya, Hasegawa, and Nakayama. Thermodynamic properties below $\sim 10T_N$ are quantitatively accounted for by this theory in its simplest form with only four parameters, which are determined by our neutron-scattering experiment. [S0163-1829(96)52530-0]

In a strongly correlated electron system, the effective mass of quasiparticles approaches infinity near the Mott transition.¹ Spin dynamics in such a ‘‘nearly localized’’ Fermi liquid are widely assumed to be described by a localized spin model, where the bandwidth for spin fluctuations is of order the exchange energy $J \sim k_B T_N$ or $k_B T_C$, where T_N or T_C is the magnetic ordering temperature. However, in the metallic state of the three-dimensional Mott compound $V_{2-y}O_3$, weak ($0.15\mu_B$ per V atom) incommensurate magnetic order was recently discovered below $T_N \approx 9$ K with overdamped spin excitations extending beyond $20k_B T_N$ in energy.² These observations suggest that even close to the metal-insulator transition, magnetism in $V_{2-y}O_3$ is itinerant and similar to that of metallic chromium.³ In this paper we examine the temperature-dependent magnetic fluctuations in metallic $V_{1.973}O_3$ and show that these and several related thermodynamic properties may be accounted for within a self-consistent renormalization theory developed to account for weak itinerant magnetism.

Itinerant or band models of magnetism, with exchange and correlation effects between opposite-spin electrons treated by the random-phase approximation (RPA), successfully describe the spin wave modes at low temperatures in iron⁴ and nickel,⁵ and capture the *qualitative* features of the overdamped spin excitations in the Stoner continuum.⁶ However, above the ordering temperature, or for the nearly or weakly itinerant antiferromagnets or ferromagnets, low-energy excitations are overdamped spin fluctuations. Coupling between these spin modes, neglected in RPA theories, needs to be considered in order to yield a coherent de-

scription of both spin fluctuations and thermodynamic properties. This is accomplished in the self-consistent renormalization (SCR) theory.⁷ The dynamic spin correlation function $S(\mathbf{q}, \omega)$ predicted by the SCR theory⁸ for nearly, or weakly, *ferromagnetic* metals was found to account for inelastic neutron scattering throughout the Brillouin zone for $\hbar\omega$ up to $8k_B T_C$ and temperature up to $10T_C$ in MnSi.⁹ Moreover, with parameters deduced from neutron scattering, the SCR theory produces quantitatively correct predictions for thermodynamic properties of the weak itinerant ferromagnets MnSi and Ni_3Al .¹⁰ An extension of the SCR theory to weak itinerant *antiferromagnetism* (AF-SCR theory) was derived by Moriya and his coworkers.¹¹ A dynamic spin correlation function of the form derived in that work has recently been used as a phenomenological model for spin fluctuations in copper oxide superconductors,¹²⁻¹⁴ but there has been no stringent experimental test of the theory.

The weak itinerant magnetism of metallic $V_{2-y}O_3$ provides an opportunity to test the ability of the AF-SCR theory to describe weak antiferromagnetism in a three-dimensional metal. In this paper we report a direct measurement of $S(\mathbf{q}, \omega)$ for metallic $V_{1.973}O_3$ by inelastic neutron scattering, with temperatures from 1.4 to 200 K. We find that the data are represented well by the AF-SCR generalized susceptibility and from the parameters derived from our measurement, the theory correctly predicts other thermodynamic properties of $V_{2-y}O_3$.

The single-crystal samples of $V_{1.973}O_3$ were grown using a skull melter and the stoichiometry was controlled to within 0.2% by annealing sliced crystals for two weeks at 1400 °C

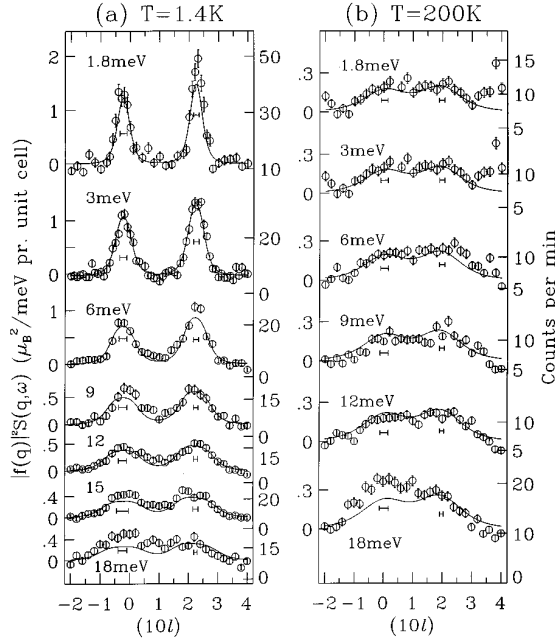


FIG. 1. Inelastic neutron scans across a whole Brillouin zone with constant energy transfer $\hbar\omega$ specified in the figure for $V_{1.973}\text{O}_3$. There are two magnetic Bragg points, $(1,0,\bar{3})$ and $(1,0,2,3)$, and two nuclear ones, $(10\bar{2})$ and (104) , within the scan range. The experimental configurations were $E_f=13.7$ meV with horizontal collimations $60^\circ-40'-40'-60'$ for $\hbar\omega=1.8-12$ meV and $E_i=35$ meV with $60^\circ-40'-60'-60'$ for $\hbar\omega=15-18$ meV. A $1''$ graphite filter was used. The horizontal bars indicate the full width at half maximum (FWHM) of the projection of the resolution function on the scan direction. The solid lines are theoretical curves $|f(\mathbf{q})|^2 S(\mathbf{q}, \omega)$ calculated from Eq. (1), where $f(\mathbf{q})$ is the V^{3+} form factor (Ref. 20).

in a suitably chosen CO-CO₂ atmosphere.¹⁵ Four single crystals were mutually aligned to increase the sensitivity of our experiment. The inelastic-neutron-scattering experiments were carried out on thermal neutron triple axis spectrometers at NIST and BNL. With appropriate resolution, magnetic neutron-scattering intensities are proportional to the dynamic spin-correlation function $S(\mathbf{q}, \omega)$. Absolute units for $S(\mathbf{q}, \omega)$ were obtained by normalizing magnetic neutron-scattering intensities to inelastic scattering from transverse acoustic phonons. Wave-vector transfer, \mathbf{q} , will be indexed in the hexagonal reciprocal lattice with $a^* = 4\pi/\sqrt{3}a = 1.47(1) \text{ \AA}^{-1}$ and $c^* = 2\pi/c = 0.448(1) \text{ \AA}^{-1}$. There are 12 V atoms in a hexagonal unit cell.²

Figure 1 shows constant energy scans for $V_{1.973}\text{O}_3$ in a wide range of energy transfer and for temperature (a) below and (b) well above T_N . The important and unusual features of the data are that (1) well within the ordered state and throughout the dominant part of the magnetic bandwidth, the peaks in $S(\mathbf{q}, \omega)$ are broad and do not bear evidence of the long-range magnetic coherence which is apparent from the magnetic Bragg peaks.² (2) The bandwidth for magnetic excitations exceeds $k_B T_N$ by more than an order of magnitude and (3) magnetic correlations persist at temperatures more than an order of magnitude larger than T_N . Figure 2 shows that the peak widths of inelastic scans, through the magnetic

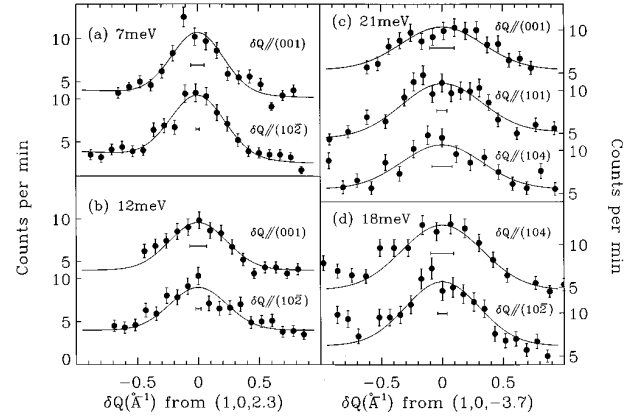


FIG. 2. Constant energy scans at 1.4 K through the magnetic reflection $(1,0,2,3)$ or $(1,0,3,7)$ along different directions within the $(h0l)$ reciprocal lattice plane. The collimations were $60^\circ-40'-40'-40'$ and $E_f=13.7$ meV for (a)–(b), and $60^\circ-40'-60'-60'$ and $E_i=35$ meV for (c)–(d). A $1''$ graphite was used as a filter. The horizontal bars indicate the FWHM of the resolution projection.

Bragg reflections $(1,0,2,3)$ and $(1,0,3,7)$ at various values of energy transfer, $\hbar\omega$, are independent of the scan directions in the $(h0l)$ zone. Because this zone contains the threefold c^* axis we conclude from this that the wave vector dependence of $S(\mathbf{q}, \omega)$ in the vicinity of magnetic Bragg reflections is approximately isotropic.

For any magnet, insulating or metallic, in which a continuous degree of freedom is broken by long-range magnetic order, the Goldstone theorem dictates that there exists a low-energy regime with gapless propagating excitations. In this spin-wave regime, the wave vector dependence of $S(\mathbf{q}, \omega)$ should display two sharp peaks on either side of the magnetic zone center which correspond to the excitation of counter-propagating spin waves. For insulating magnets, the spin-wave regime covers an energy range of order $k_B T_N$ and most of the spectral weight is associated with spin waves. For itinerant magnets on the other hand, spin waves only exist in a limited low-energy regime beyond which they merge with Stoner continuum. Our data show that $V_{1.973}\text{O}_3$ is a rather extreme case in which the dominant part of the magnetic spectral weight is associated with magnetic excitations in the Stoner continuum. Concomitantly the long-range ordered staggered magnetic moment, $M_{\mathbf{Q}}$, as well as T_N are anomalously small compared to the total spin on a V ion and the magnetic bandwidth, respectively.

Although $V_{1.973}\text{O}_3$ is near the boundary of a metal-insulator transition, our data clearly demonstrates that magnetism in this material cannot be accounted for by local moment theories. Instead we find that the AF-SCR theory¹¹ describes our data very well. In that theory, the imaginary part of the generalized susceptibility, which is related to the dynamic spin correlation function measured through neutron scattering by $S(\mathbf{q}, \omega) \equiv \pi^{-1} \langle n(\omega) + 1 \rangle \chi''(\mathbf{q}, \omega)$, is given by

$$\chi''(\mathbf{Q}+\mathbf{q}, \omega) = \chi_{\mathbf{Q}} \frac{\hbar\omega/\Gamma\kappa^2}{(\hbar\omega/\Gamma\kappa^2)^2 + [1 + (q/\kappa)^2]^2} \quad (1)$$

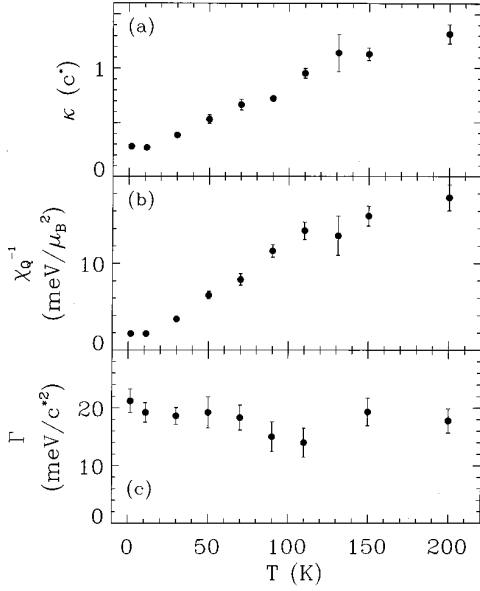


FIG. 3. The parameters of the AF-SCR theory for $V_{1.973}O_3$, determined at various temperatures from the measured dynamic spin correlation function. Units in (b) are per vanadium atom (Ref. 17).

where \mathbf{Q} is the AF wave vector which is near $(1,0,2.3)$ or $(1,0,0.3)$ in the present case, $\chi_{\mathbf{Q}}$ is the static staggered susceptibility, κ is the characteristic width in \mathbf{k} space and Γ is a temperature-insensitive parameter. The energy scale is $\Gamma\kappa^z$ with a dynamic exponent $z=2$, reflecting the strong damping of spin excitations in the Stoner continuum. This functional form for $\chi''(\mathbf{Q}+\mathbf{q},\omega)$ describes our data very well as may be appreciated by inspecting Fig. 1 in which the solid lines are the result of a least squares fit to the theoretical form.¹⁶ From such fits to a complete set of constant energy scans at one temperature, we extract three parameters, κ , $\chi_{\mathbf{Q}}$, and Γ .

The SCR theory predicts the temperature dependence of κ , $\chi_{\mathbf{Q}}$, and Γ . To test these predictions, we performed a complete measurement of $S(\mathbf{q},\omega)$ at a number of temperatures and Fig. 3 shows the temperature-dependent parameters which we extracted from the data by fitting to Eq. (1). The characteristic width κ increases monotonically with temperature and has a finite value at $T=0$. Γ is temperature insensitive [Fig. 3(c)] and therefore the temperature variation of the characteristic energy, $\Gamma\kappa^2$, is determined by that of κ . All these results are anticipated by the AF-SCR theory which also predicts Curie-Weiss-like behavior for the staggered susceptibility $\chi_{\mathbf{Q}}$ which is consistent with our data for temperatures up to ~ 100 K [Fig. 3(b)]. Unlike in a localized spin model, this Curie-Weiss-like behavior is attributed to the temperature dependence of the instantaneous local fluctuating moment $\Sigma_{\mathbf{q}}(|M_{\mathbf{q}}|^2)$.⁸ Saturation of $1/\chi_{\mathbf{Q}}$ at high temperatures is an indication of strong mode-mode coupling.¹¹ Comparing the measured $1/\chi_{\mathbf{Q}}$ vs T curve with numerical solutions in Ref. 11, the coupling constant \bar{F}_S was estimated to be of the order of $10^{1.5}$ meV/ μ_B^4 .

The SCR theory is represented by a set of integrodifferential equations, which in general can only be solved numerically. In the low-temperature regime, however, simplifi-

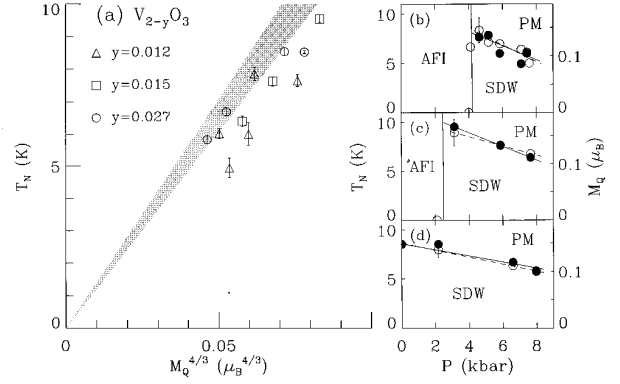


FIG. 4. (b)–(d) show the Néel temperature (dots, left scale) and the staggered moment at 1.5 K (circles, right scale) for the spin density wave (SDW) as function of pressure for $V_{2-y}O_3$ with $y=0.012$, 0.015 , and 0.027 , respectively. PM stands for paramagnetic metallic phase and AFI for antiferromagnetic insulating phase. For the first two compositions, pressure is required to stabilize the metallic state. For the last one, the material is metallic at ambient pressure. (a) shows T_N vs $M_{\mathbf{Q}}^{3/4}$ with pressure and composition as implicit variables. The hatched line is the prediction of the AF-SCR theory, using Γ and \bar{A} determined from spin fluctuations.

cation is possible. Apart from Γ , \bar{F}_S , and the saturated staggered moment, $M_{\mathbf{Q}}$, the AF-SCR theory in its simplest form needs only one more constant, $\bar{A} \equiv (\chi_{\mathbf{Q}}\kappa^2)^{-1}$, to determine the temperature dependence of most thermodynamic properties.¹¹ Our experimental values of $(\chi_{\mathbf{Q}}\kappa^2)^{-1}$ shows a deviation from its low temperature value above 100 K which marks the upper limit of validity for this simplified four parameter [$M_{\mathbf{Q}}=0.15\mu_B$ per V,² $\Gamma=19$ meV/ c^2 ,² $\bar{A}=24$ meV/ $(\mu_B c^*)^2$ per V, and $\bar{F}_S=30$ meV/ μ_B^4] AF-SCR theory. The theory predicts a linear in T contribution to the specific heat due to spin fluctuations with a Sommerfeld constant $\gamma_m \equiv \frac{3}{2}\alpha\pi N k_B^2 / (\Gamma q_B^2)$ where N is the number of V atoms, q_B is the cutoff wave vector and $\alpha \leq 2$ is a numerical factor.^{18,13} Using $\alpha=2$ and $q_B=(6\pi^2/v_0)^{1/3}$ with the volume per atom $v_0=24.6 \text{ \AA}^3$, $\gamma_m \approx 39$ mJ/K²mole V. This magnetic contribution to the electronic specific heat accounts for a large part of the measured $\gamma=54\text{--}70$ mJ/K²mole V.¹⁹ The predicted Néel temperature¹³ $T_N \equiv 0.7137(\bar{A}\Gamma^{1/2}M_{\mathbf{Q}}^2/v_0)^{2/3}/k_B \approx 10$ K, agrees excellently with the observed value $T_N \approx 9$ K. An additional test of the expression for T_N is provided by measurements of T_N and $M_{\mathbf{Q}}$ versus hydrostatic pressure.²¹ Hydrostatic pressure suppresses both these variables as it drives the material more metallic. As \bar{A} and Γ both are T independent for $T < 100$ K, we may also expect them to be pressure insensitive in which case $T_N \propto M_{\mathbf{Q}}^{4/3}$. In Fig. 4, we show that this relation is in fact obeyed very closely for $P < 8$ kbar.

The temperature dependence of the staggered magnetization, $M_{\mathbf{Q}}^2(T)$, within the AF-SCR theory can vary from $T^{3/2}$ to T^2 depending on the values of $\xi \equiv \bar{F}_S M_{\mathbf{Q}}^2 / \bar{A} q_B^2$ and $\eta \equiv \bar{F}_S \Gamma / \bar{A}^2 q_B^2$.¹¹ A numerical solution of the AF-SCR equations corresponding to our values of ξ and η is not currently available but for future comparison, we present our measurements of $M_{\mathbf{Q}}^2(T)$ in Fig. 5. The AF-SCR theory also relates

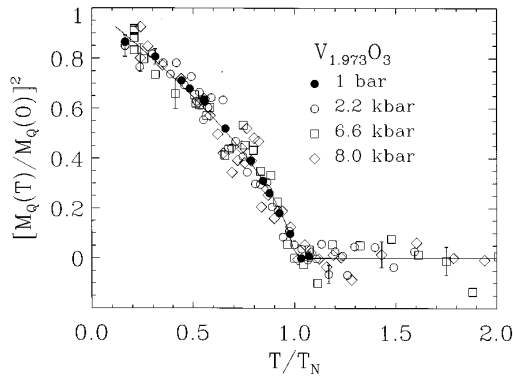


FIG. 5. Normalized intensity of the antiferromagnetic Bragg peak (1,0,2.3), probing $M_{\mathbf{Q}}^2(T)/M_{\mathbf{Q}}^2(0)$ vs the reduced temperature T/T_N for a $V_{1.973}O_3$ sample at various values of hydrostatic pressure. The normalized order parameter curves are indistinguishable for $P < 8$ kbar. The solid line is $M_{\mathbf{Q}}^2(T)/M_{\mathbf{Q}}^2(0) = (1 - T/T_N)^{2\beta}$ with $2\beta = 0.63$.

the T -dependent staggered magnetization $M_{\mathbf{Q}}(T)$ to thermal expansion of magnetic origin below T_N ,¹¹ however, no thermal expansion data on $V_{2-y}O_3$ is currently available.

The four SCR parameters, $M_{\mathbf{Q}}, \Gamma, A$, and \bar{F}_S , can be calculated from a Hubbard-like microscopic model.¹¹ With our measurement of their values, the tight-binding and correlation parameters of a microscopic model, in principle, can be determined for metallic $V_{2-y}O_3$. Metals close to antiferromagnetic instabilities have been the subject of recent interest in the context of quantum critical phenomena.^{22,23} For a three-dimensional itinerant system with a magnetic wave

vector away from Fermi surface nesting, there exist, apart from the ordered phase, the so-called classical Gaussian, perturbative Gaussian, and disordered quantum regimes. The SCR theory has been shown to represent the classical Gaussian regime.²³ An extension of the SCR theory to systems with a nesting Fermi surface appeared recently.²⁴

In summary, spin fluctuations in the doped Mott compound $V_{1.973}O_3$ are isotropic in \mathbf{k} space and centered around antiferromagnetic Bragg reflections with a magnetic bandwidth which exceeds $20k_B T_N$. These overdamped but spatially correlated itinerant magnetic fluctuations persist up to temperatures 20 times larger than T_N . Our experimental results contradict the widely circulated belief that spin fluctuations on both sides of a Mott metal-insulator transition can be described by a localized spin model, where the bandwidth of the spin fluctuations is set by $k_B T_N$ and where spin fluctuations near the magnetic zone centers disappear rapidly above T_N . Instead spin fluctuations in $V_{1.973}O_3$ for temperatures and energies up to $20T_N$ are well described by the dynamic susceptibility of the SCR theory. For temperatures below $\sim 10T_N$ we have shown that the SCR theory, based on four parameters which are extracted from neutron-scattering data, correctly predicts T_N and accounts for most of the enhanced low-temperature electronic specific heat.

Discussions and communications with G. Aeppli, A. Fujimori, A. J. Millis, Q. M. Si, S. Sachdev, R. J. Birgeneau, T. Moriya, and S. M. Shapiro are gratefully acknowledged. W.B. acknowledges the Aspen Center for Physics where part of this work was performed. Work at JHU was supported by Grant No. DMR-9453362, at BNL was supported by DOE under Contract No. DE-AC02-76CH00016 and J.M.H. was supported by MISCON Grant No. DE-FG02-90ER45427.

¹W. F. Brinkman and T. M. Rice, Phys. Rev. B **2**, 4302 (1970); Y. Tokura *et al.*, Phys. Rev. Lett. **70**, 2126 (1993).
²W. Bao *et al.*, Phys. Rev. Lett. **71**, 766 (1993).
³E. Fawcett, Rev. Mod. Phys. **60**, 209 (1988).
⁴J. W. Lynn, Phys. Rev. B **11**, 2624 (1975); J. F. Cooke, J. W. Lynn, and H. L. Davis, *ibid.* **21**, 4118 (1980).
⁵H. A. Mook and D. McK. Paul, Phys. Rev. Lett. **54**, 227 (1985); J. F. Cooke *et al.*, *ibid.* **54**, 718 (1985).
⁶Y. Ishikawa *et al.*, Phys. Rev. B **16**, 4956 (1977).
⁷K. K. Murata and S. Doniach, Phys. Rev. Lett. **29**, 285 (1972); T. Moriya and A. Kawabata, J. Phys. Soc. Jpn. **34**, 639 (1973); **35**, 669 (1973).
⁸T. Moriya, *Spin Fluctuations in Itinerant Electron Magnetism* (Springer-Verlag, Berlin, 1985).
⁹Y. Ishikawa *et al.*, Phys. Rev. B **25**, 254 (1982); **31**, 5884 (1985).
¹⁰Y. Takahashi and T. Moriya, J. Phys. Soc. Jpn. **54**, 1592 (1985); G. G. Lonzarich, J. Magn. Magn. Mater. **45**, 43 (1984); N. R. Bernhoeft *et al.*, Phys. Rev. B **28**, 422 (1983).
¹¹H. Hasegawa and T. Moriya, J. Phys. Soc. Jpn. **36**, 1542 (1974); K. Nakayama and T. Moriya, *ibid.* **56**, 2918 (1987).
¹²A. J. Millis, H. Monien, and D. Pines, Phys. Rev. B **42**, 167 (1990); T. Moriya, Y. Takahashi, and K. Ueda, J. Phys. Soc. Jpn. **59**, 2905 (1990); P. Monthoux and D. Pines, Phys. Rev. B **47**, 6069 (1993).

¹³T. Moriya and K. Ueda, J. Phys. Soc. Jpn. **63**, 1871 (1994).
¹⁴T. E. Mason, G. Aeppli, and H. A. Mook, Phys. Rev. Lett. **68**, 1414 (1992). Their notations $\chi^0/\kappa^2, A^2$, and κ correspond to our $\chi_{\mathbf{Q}}, \Gamma$, and κ of Eq. (1).
¹⁵J. E. Keem *et al.*, Am. Ceram. Soc. Bull. **56**, 1022 (1977); H. R. Harrison *et al.*, Mater. Res. Bull. **15**, 571 (1980); S. A. Shivasankar *et al.*, J. Electrochem. Soc. **128**, 2472 (1981); **129**, 1641 (1982).
¹⁶Extra intensity near (100) for 18 meV is due to the direct beam when scattering angle is small.
¹⁷Unit per V atom was converted from unit per unit cell by dividing with the squared structure factor $|\mathcal{F}(\mathbf{Q})|^2 = 28.5$ and 20.0 (Ref. 2) for $\mathbf{Q} = (1,0,2.3)$ and $(1,0,0.3)$, respectively.
¹⁸H. Hasegawa, J. Phys. Soc. Jpn. **38**, 107 (1975).
¹⁹D. B. McWhan *et al.*, Phys. Rev. B **7**, 326 (1973); S. A. Carter *et al.*, *ibid.* **48**, 16 841 (1993).
²⁰R. E. Watson and A. J. Freeman, Acta Crystallogr. **14**, 27 (1961).
²¹High-pressure apparatus was described in W. Bao, C. Broholm, and S. F. Trevino, Rev. Sci. Instrum. **66**, 1260 (1995). Helium was used as the pressure transducer.
²²S. Sachdev and J. Ye, Phys. Rev. Lett. **69**, 2411 (1992); A. V. Chubukov and S. Sachdev, *ibid.* **71**, 169 (1993).
²³A. J. Millis, Phys. Rev. B **48**, 7183 (1993).
²⁴O. Narikiyo and K. Miyake, J. Phys. Soc. Jpn. **64**, 2730 (1995).